arXiv:1512.06029v2 [cond-mat.quant-gas] 16 Mar 2016

Physical dipoles and second order perturbation theory for dipolar fermions in two dimensions

Philipp Lange, Jan Krieg, and Peter Kopietz
Institut für Theoretische Physik, Universität Frankfurt, Max-von-Laue Strasse 1, 60438 Frankfurt, Germany
(Dated: March 17, 2016)

In two dimensions the Fourier transform of the interaction between two point dipoles has a term which grows linearly in the modulus $|\boldsymbol{q}|$ of the momentum. As a consequence, in second order perturbation theory the self-energy of two-dimensional dipolar fermions is ultraviolet divergent. We show that for electric dipoles this divergence can be avoided if one takes into account that physical dipoles consist of two opposite charges which are separated by a finite distance. Using this regularization, we calculate the self-energy, the renormalized chemical potential, and the renormalized Fermi surface of dipolar fermions in two dimensions in second order perturbation theory. We find that in the Fermi liquid phase the second order corrections weaken first order effects.

PACS numbers: 03.75.Ss, 67.85.-d, 71.10.Ay

I. INTRODUCTION

In the last decade many-body systems consisting of fermionic atoms or molecules which carry a finite electric or magnetic dipole moment have been intensely studied both experimentally[1–16] and theoretically[17–40]. In these systems the spatially anisotropic nature of the dipole-dipole interaction gives rise to a rather complex phase diagram, which includes a normal Fermi liquid phase and phases with spontaneously broken symmetries, such as superfluid, magnetic, and nematic phases. Experimentally, many-body systems of fermions coupled by dipolar forces have been realized both in two and three dimensions. Here we shall focus on many-body corrections to the single-particle spectrum in the normal Fermi liquid phase of dipolar fermions in two spatial dimensions (2D). Specifically, we shall calculate the irreducible self-energy $\Sigma(\boldsymbol{k},\omega)$ as a function of momentum $\boldsymbol{k}$ and frequency ω up to second order perturbation theory and determine the renormalized Fermi surface to this order. Recently we have performed analogous calculations for dipolar fermions in three dimensions[37]. However, these calculations cannot be simply extended to the two-dimensional case because in 2D the self-energy $\Sigma(\boldsymbol{k},\omega)$ is ultraviolet divergent. This divergence is due to the fact that in momentum space the 2D Fourier transform of the dipolar interaction contains a term which grows linearly with the modulus of the momentum. While several regularization strategies have been proposed in the literature[41,42], we show here that all divergences can be avoided if one replaces the point dipoles by physical dipoles. In the electric case, we therefore replace each point dipole by two opposite charges which are separated by a finite distance $\boldsymbol{\ell}$. Using this regularization, we shall in this work calculate the self-energy, the renormalized chemical potential, and the renormalized Fermi surface of two-dimensional dipolar fermions in second order perturbation theory.

II. REGULARIZATION OF THE DIPOLAR INTERACTION IN 2D: PHYSICAL DIPOLES

Consider a many-body system consisting of spinless fermionic atoms or molecules with mass m and a finite dipole moment $\boldsymbol{d}$. Assuming that the particles are confined to the xy-plane and that all dipoles are aligned by an external field, the second-quantized Hamiltonian of the system is

$$\mathcal{H} = \int d^2r\, \hat{\psi}^\dagger(\boldsymbol{r}) \left(-\frac{\nabla^2}{2m}\right) \hat{\psi}(\boldsymbol{r}) + \frac{1}{2}\int d^2r \int d^2r'\, \hat{\psi}^\dagger(\boldsymbol{r})\hat{\psi}(\boldsymbol{r})U(\boldsymbol{r}-\boldsymbol{r'})\hat{\psi}^\dagger(\boldsymbol{r'})\hat{\psi}(\boldsymbol{r'}), \tag{1}$$

where $\hat{\psi}^\dagger(\boldsymbol{r})$ and $\hat{\psi}(\boldsymbol{r})$ are the usual field operators which create or annihilate a fermion at position $\boldsymbol{r} = r_x\hat{\boldsymbol{x}}+r_y\hat{\boldsymbol{y}}$ in the xy-plane, and we have set $\hbar = 1$. Here the orthogonal unit vectors $\hat{\boldsymbol{x}}$ and $\hat{\boldsymbol{y}}$ form a basis in the xy-plane. The dipole-dipole interaction between two point dipoles with dipole moment $\boldsymbol{d}$ which are separated by the vector $\boldsymbol{r}$ is given by

$$U(\boldsymbol{r}) = \frac{d^2}{|\boldsymbol{r}|^3}\left[1-3(\hat{\boldsymbol{d}}\cdot\hat{\boldsymbol{r}})^2\right], \tag{2}$$

where $\hat{\boldsymbol{d}} = \boldsymbol{d}/|\boldsymbol{d}|$ and $\hat{\boldsymbol{r}} = \boldsymbol{r}/|\boldsymbol{r}|$ are unit vectors. Expanding the field operators in momentum space, $\hat{\psi}(\boldsymbol{r}) = \frac{1}{\sqrt{V}}\sum_{\boldsymbol{k}} e^{i\boldsymbol{k}\cdot\boldsymbol{r}}c_{\boldsymbol{k}}$, where V is the (two-dimensional) volume of the system, our Hamiltonian (1) can be written as

$$\mathcal{H} = \sum_{\boldsymbol{k}} \frac{\boldsymbol{k}^2}{2m} c^\dagger_{\boldsymbol{k}} c_{\boldsymbol{k}} + \frac{1}{2V}\sum_{\boldsymbol{k},\boldsymbol{k'q}} U_{\boldsymbol{q}} c^\dagger_{\boldsymbol{k}+\boldsymbol{q}} c^\dagger_{\boldsymbol{k'}-\boldsymbol{q}} c_{\boldsymbol{k'}} c_{\boldsymbol{k}}, \tag{3}$$

where the two-dimensional Fourier transform of the dipolar interaction is defined by

$$U_{\boldsymbol{q}} = \int d^2r e^{-i\boldsymbol{q}\cdot\boldsymbol{r}} U(\boldsymbol{r}). \tag{4}$$

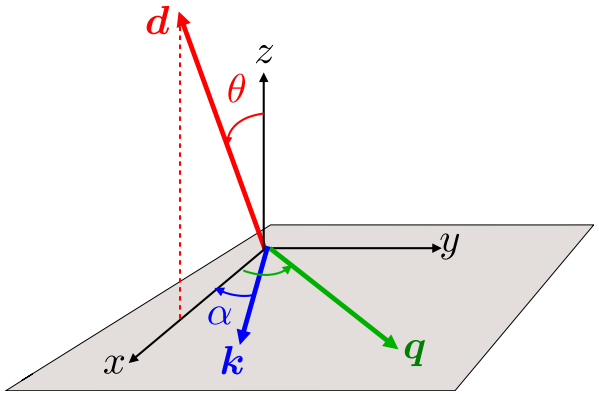

FIG. 1. (Color online) For a two-dimensional system of dipoles $\boldsymbol{d}$ with arbitrary orientation, we choose our coordinate system such that the particles move in the xy-plane and $\boldsymbol{d}$ lies in the xz-plane. The momentum transferred by the interaction is denoted by $\boldsymbol{q}$. For later reference, we have also indicated the momentum $\boldsymbol{k}$ of a quasi-particle.

As it stands, Eq. (4) is ultraviolet divergent and has to be regularized. One possibility is to exclude the short-distance regime $|\boldsymbol{r}| < r_0$ from the $\boldsymbol{r}$-integration. This regularization has been introduced in Ref. [42]. The integral is then finite and one obtains the regularized Fourier transform of the dipolar interaction in 2D for small momenta $|\boldsymbol{q}| \ll 1/r_0$,

$$\begin{aligned} U_{\boldsymbol{q}}^{(r_0)} &= \int_{|\boldsymbol{r}|>r_0} d^2 r e^{-i\boldsymbol{q}\cdot\boldsymbol{r}} U(\boldsymbol{r}) \\ &\approx -\frac{\pi d^2}{r_0}\left[1-3\cos^2\theta\right] \\ &\quad -2\pi d^2|\boldsymbol{q}|\left[\cos^2\theta-(\hat{\boldsymbol{x}}\cdot\hat{\boldsymbol{q}})^2\sin^2\theta\right], \end{aligned} \tag{5}$$

where θ is the angle between $\boldsymbol{d}$ and the z-axis and we have oriented our coordinate system in the xy-plane such that $\boldsymbol{d}$ lies in the xz-plane, as shown in Fig. 1. Although the first term in Eq. (5) explicitly depends on the cutoff r_0, this term corresponds to a contact interaction and does not affect the physics of a one-component Fermi gas. Keeping in mind that the linear increase of the second term in Eq. (5) should be cut off at $|\boldsymbol{q}| \approx 1/r_0$, perturbation theory with the interaction $U_{\boldsymbol{q}}^{(r_0)}$ is ultraviolet convergent; however, physical quantities which depend on short-distance physics can exhibit a rather complicated dependence on r_0.

The above complications can be avoided if one uses the regularization procedure proposed by Fischer[41] who proposed to consider a quasi-two-dimensional system where the dipoles are confined to the lowest transverse subband due to an external harmonic confining potential in z-direction. If the trapping frequency ω_z of the confining potential is larger than the chemical potential μ and the temperature T, the particles occupy only the lowest transverse subband with wavefunction

$$\phi_0(z) = \pi^{-1/4} a^{-1/2} e^{-z^2/(2a^2)}. \tag{6}$$

The length scale a is defined by the trapping frequency ω_z and is given by $a = (m\omega_z)^{-1/2}$. One then convolutes the three-dimensional dipolar interaction $U(\boldsymbol{r}-\boldsymbol{r}', z-z')$ with the probability density profile in the transverse direction,

$$U^{(a)}(\boldsymbol{r}) = \int dz \int dz' \phi_0(z)^2 \phi_0(z')^2 U(\boldsymbol{r}, z-z'). \tag{7}$$

The integration can be carried out exactly; Fourier transforming the result to momentum space one obtains for the regularized effective 2D dipolar interaction

$$\begin{aligned} U_{\boldsymbol{q}}^{(a)} &= -\frac{\sqrt{2\pi}d^2}{a}\left[1-3\cos^2\theta\right] \\ &\quad -\frac{2\pi d^2}{a} F(|\boldsymbol{q}|a)\left[\cos^2\theta-(\hat{\boldsymbol{x}}\cdot\hat{\boldsymbol{q}})^2\sin^2\theta\right], \end{aligned} \tag{8}$$

where the dimensionless function $F(x)$ can be expressed in terms of the complementary error function $\mathrm{Erfc}(x)$ as follows,

$$F(x) = x e^{x^2/2} \mathrm{Erfc}(x/\sqrt{2}). \tag{9}$$

Note that $F(x) \sim x$ for small x so that in the long-wavelength regime $|\boldsymbol{q}| \ll 1/a$ the momentum-dependent part of $U_{\boldsymbol{q}}^{(a)}$ agrees precisely with the momentum-dependent part of $U_{\boldsymbol{q}}^{(r_0)}$ in Eq. (5). On the other hand, using the fact that $F(x) \sim \sqrt{2/\pi} + \mathcal{O}(x^{-2})$ for large x, we see that for $|\boldsymbol{q}| \gg 1/a$ the regularized interaction $U_{\boldsymbol{q}}^{(a)}$ approaches a finite limit,

$$\lim_{|\boldsymbol{q}|\to\infty} U_{\boldsymbol{q}}^{(a)} = \frac{\sqrt{2\pi}d^2}{a}\left[2(\hat{\boldsymbol{x}}\cdot\hat{\boldsymbol{q}})^2-1\right]\sin^2\theta, \tag{10}$$

which is independent of $|\boldsymbol{q}|$ but still depends on the direction $\hat{\boldsymbol{q}}$. The above regularization of the dipolar interaction in two dimensions has recently been used by several authors[17,26,36,43–45].

Let us now propose a different regularization procedure which does not require the embedding of the system into a harmonic trapping potential and has the advantage that the Fourier transform of the regularized interaction vanishes for large momentum transfers. For simplicity, we focus on electric dipoles. A generalization to magnetic dipoles seems to be possible, although we have not attempted to work out the details. The crucial point is that a physical electric dipole consists of two opposite point charges $\pm Q$ which are separated by a finite distance $\boldsymbol{\ell}$.[46] The corresponding electric dipole moment is $\boldsymbol{d} = Q\boldsymbol{\ell}$. The three-dimensional charge density at position $\boldsymbol{R}$ of N aligned electric dipoles whose center is located at positions $\boldsymbol{R}_i$ is therefore given by

$$\begin{aligned} \rho^{(3)}(\boldsymbol{R}) = Q\sum_{i=1}^{N}\big[&\delta^{(3)}(\boldsymbol{R}-\boldsymbol{R}_i-\boldsymbol{\ell}/2) \\ &-\delta^{(3)}(\boldsymbol{R}-\boldsymbol{R}_i+\boldsymbol{\ell}/2)\big], \end{aligned} \tag{11}$$

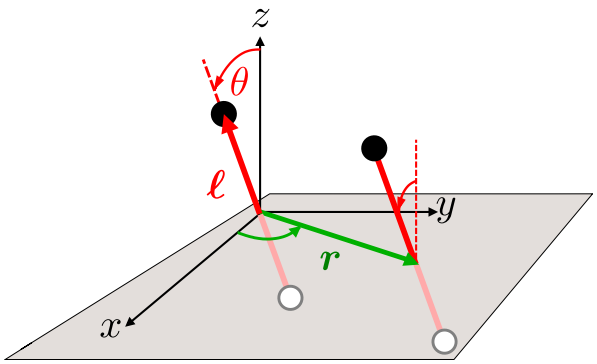

FIG. 2. (Color online) Sketch of two aligned dipoles in real space. The displacement vector $\boldsymbol{\ell}$ lies in the xz-plane and the vector $\boldsymbol{r}$, separating the two dipoles, lies in the xy-plane. The black and white dots represent the charges of the dipole.

where $\delta^{(3)}(\boldsymbol{R})$ is the three-dimensional Dirac δ-distribution. The electrostatic Coulomb energy stored in this charge distribution is

$$E_{\rm el} = \frac{1}{2}\int d^3R \int d^3R' \frac{\rho^{(3)}(\boldsymbol{R})\rho^{(3)}(\boldsymbol{R}')}{|\boldsymbol{R}-\boldsymbol{R}'|}. \qquad (12)$$

Suppose now that the centers of all dipoles are located in the xy-plane and that all dipole moments are aligned and lie in the xz-plane, as shown in Fig. 2. The positions of the centers of the dipoles are then of the form $\boldsymbol{R}_i = \boldsymbol{r}_i$, where the vector $\boldsymbol{r}_i$ has no components in z-direction. Setting $\boldsymbol{R} = \boldsymbol{r} + z\hat{\boldsymbol{z}}$ and $\boldsymbol{R}' = \boldsymbol{r}' + z'\hat{\boldsymbol{z}}$ in Eq. (12), where $\boldsymbol{r}$ and $\boldsymbol{r}'$ lie now in the xy-plane, and integrating over z and z' we can rewrite the electrostatic interaction energy of the dipoles in the form

$$\begin{aligned} E_{\rm el} &= \frac{Q^2}{2}\sum_{ij}\left[\frac{2}{|\boldsymbol{r}_i-\boldsymbol{r}_j|} - \frac{1}{|\boldsymbol{r}_i-\boldsymbol{r}_j+\boldsymbol{\ell}|} - \frac{1}{|\boldsymbol{r}_i-\boldsymbol{r}_j-\boldsymbol{\ell}|}\right] \\ &= \frac{1}{2}\int d^2r \int d^2r' \rho(\boldsymbol{r}) U^{(\ell)}(\boldsymbol{r}-\boldsymbol{r}')\rho(\boldsymbol{r}'), \qquad (13) \end{aligned}$$

where

$$\rho(\boldsymbol{r}) = \sum_{i=1}^{N}\delta^{(2)}(\boldsymbol{r}-\boldsymbol{r}_i) \qquad (14)$$

is the two-dimensional density of dipoles and

$$U^{(\ell)}(\boldsymbol{r}) = Q^2\left[\frac{2}{|\boldsymbol{r}|} - \frac{1}{|\boldsymbol{r}+\boldsymbol{\ell}|} - \frac{1}{|\boldsymbol{r}-\boldsymbol{\ell}|}\right] \qquad (15)$$

is the regularized dipole-dipole interaction. In the isotropic case ($\theta = 0$) this reduces to the interaction used in Ref. [34] to study Wigner crystallization in two dimensions. The two-dimensional Fourier transform of Eq. (15) is

$$U_{\boldsymbol{q}}^{(\ell)} = \frac{4\pi Q^2}{|\boldsymbol{q}|}\left[1 - e^{-\ell|\boldsymbol{q}||\cos\theta|}\cos(\boldsymbol{q}\cdot\hat{\boldsymbol{x}}\,\ell\sin\theta)\right], \qquad (16)$$

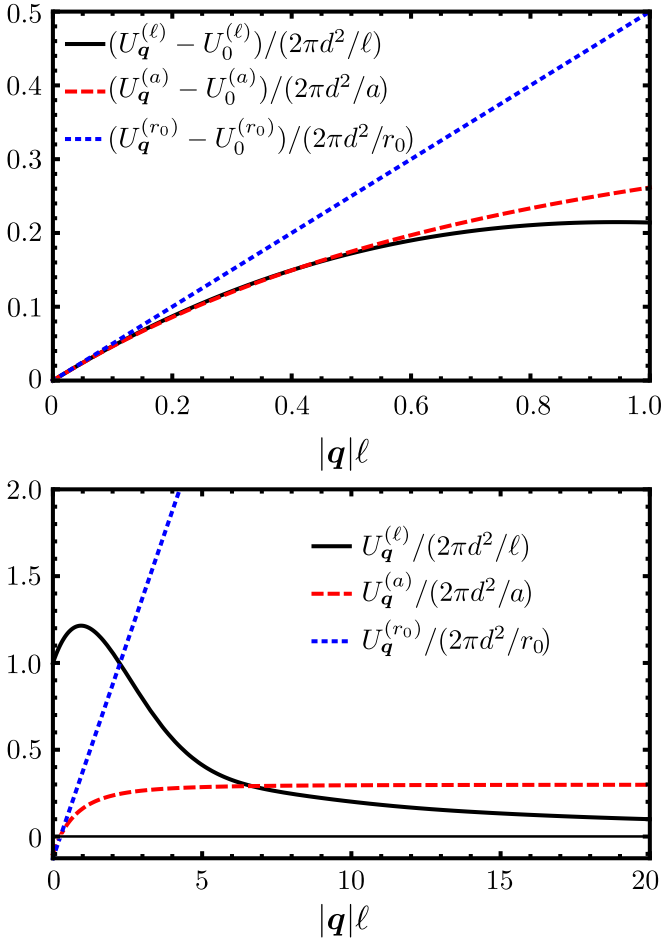

FIG. 3. (Color online) Plot of the Fourier transform of the dipole-dipole interaction for tilt angle $\theta = \pi/3$ and $\hat{\boldsymbol{q}}\cdot\hat{\boldsymbol{x}} = 1$ against $|\boldsymbol{q}|\ell$ for all three regularization strategies discussed in Sec. II; $U_{\boldsymbol{q}}^{(\ell)}$ (black solid line), $U_{\boldsymbol{q}}^{(a)}$ (red dashed line), and $U_{\boldsymbol{q}}^{(r_0)}$ (blue dotted line). To compare the regularization strategies we set $r_0 = a = \ell$. The upper panel shows the behavior for small $|\boldsymbol{q}|\ell$ where we have shifted $U_{\boldsymbol{q}}$ by U_0 for better comparison. In the lower panel we plot $U_{\boldsymbol{q}}$ in a larger momentum range.

where θ is again the angle between the direction of the dipole and the z-axis, see Fig. 2. Keeping in mind that $Q = d/\ell$ and expanding the term in the square brackets of Eq. (16) up to second order in $|\boldsymbol{q}|$ we obtain

$$\begin{aligned} U_{\boldsymbol{q}}^{(\ell)} &= \frac{4\pi d^2}{\ell}|\cos\theta| \\ &\quad - 2\pi d^2|\boldsymbol{q}|\left[\cos^2\theta - (\hat{\boldsymbol{x}}\cdot\hat{\boldsymbol{q}})^2\sin^2\theta\right] + \mathcal{O}(\boldsymbol{q}^2). \qquad (17) \end{aligned}$$

Obviously, the leading order momentum-dependent term agrees with the momentum-dependent term of $U_{\boldsymbol{q}}^{(r_0)}$ in Eq. (5). On the other hand, for $|\boldsymbol{q}| \gg 1/\ell$ the regularized Fourier transform (16) vanishes as $4\pi Q^2/|\boldsymbol{q}|$, which is just the bare Coulomb interaction between the charges attached to two dipoles. The $1/|\boldsymbol{q}|$ decay of the interaction for large momenta guarantees that perturbation theory in powers of $U_{\boldsymbol{q}}^{(\ell)}$ is ultraviolet convergent. In Fig. 3 we

compare the momentum dependence of the three different regularized dipolar interactions given in Eqs. (5), (8) and (16). Once we subtract the regularization dependent constants $U_0^{(\ell)}$, $U_0^{(a)}$, or $U_0^{(r_0)}$, the behavior for $|q| \ll 1/\ell$ is very similar for all three regularization strategies. Since we consider a one-component Fermi gas the self-energy does not depend on these constants. However, for large momenta $U_{\boldsymbol{q}}^{(\ell)}$ vanishes as $|\boldsymbol{q}|^{-1}$, whereas $U_{\boldsymbol{q}}^{(r_0)}$ grows linearly, and $U_{\boldsymbol{q}}^{(a)}$ approaches a finite limit which depends on θ and $\hat{\boldsymbol{q}}$.

III. RENORMALIZED FERMI SURFACE AND CHEMICAL POTENTIAL

In this section we will work with the regularization via physical dipoles $U_{\boldsymbol{q}}^{(\ell)}$. For convenience we rename $U_{\boldsymbol{q}}^{(\ell)} \to U_{\boldsymbol{q}}$, i.e., we omit the superscript indicating the regularization dependence of the interaction. In the normal Fermi liquid phase, the self-energy of dipolar fermions up to second order in the interaction is in the thermodynamic limit and at vanishing temperature given by[37]

$$\Sigma(\boldsymbol{k}, i\omega) = \Sigma_1(\boldsymbol{k}) + \Sigma_2(\boldsymbol{k}, i\omega), \tag{18}$$

where the first order correction is

$$\Sigma_1(\boldsymbol{k}) = \int_{\boldsymbol{q}} (U_0 - U_{\boldsymbol{q}})\Theta(-\xi_{\boldsymbol{k}+\boldsymbol{q}}), \tag{19}$$

and the second order term is

$$\begin{aligned}\Sigma_2(\boldsymbol{k}, i\omega) = &-\int_{\boldsymbol{q}}\int_{\boldsymbol{q}'} (U_0 - U_{\boldsymbol{q}})(U_0 - U_{\boldsymbol{q}'})\Theta(-\xi_{\boldsymbol{q}+\boldsymbol{q}'})\delta(\xi_{\boldsymbol{q}'+\boldsymbol{k}}) \\ &+ \frac{1}{2}\int_{\boldsymbol{q}}\int_{\boldsymbol{q}'} [U_{\boldsymbol{q}} - U_{\boldsymbol{q}'}]^2 \frac{\Theta(\xi_{\boldsymbol{k}+\boldsymbol{q}})\Theta(\xi_{\boldsymbol{k}+\boldsymbol{q}'})\Theta(-\xi_{\boldsymbol{k}+\boldsymbol{q}+\boldsymbol{q}'}) + \Theta(-\xi_{\boldsymbol{k}+\boldsymbol{q}})\Theta(-\xi_{\boldsymbol{k}+\boldsymbol{q}'})\Theta(\xi_{\boldsymbol{k}+\boldsymbol{q}+\boldsymbol{q}'})}{i\omega - (\xi_{\boldsymbol{k}+\boldsymbol{q}} + \xi_{\boldsymbol{k}+\boldsymbol{q}'} - \xi_{\boldsymbol{k}+\boldsymbol{q}+\boldsymbol{q}'})}.\end{aligned} \tag{20}$$

Here $\int_{\boldsymbol{q}} = \int d^2q/(2\pi)^2$ and $\xi_{\boldsymbol{k}} = \boldsymbol{k}^2/(2m) - \mu$ is the bare energy relative to the chemical potential μ. The first term in Eq. (20) arises from the iteration of the first order self-energy, while the frequency-dependent term in the second line corresponds to the second order contributions which cannot be generated by iterating first order corrections.

We have calculated the above self-energies numerically using the VEGAS Monte Carlo algorithm from the GNU Scientific Library[47] for the numerical integrations in C++. Given the self-energy $\Sigma(\boldsymbol{k}_F, 0)$ at vanishing frequency, we can determine the renormalized Fermi surface by solving the implicit equation

$$\frac{k_F^2}{2m} + \Sigma(\boldsymbol{k}_F, 0) = \mu. \tag{21}$$

It is convenient to parametrize the renormalized Fermi surface in terms of polar coordinates, $\boldsymbol{k}_F = k_F(\alpha)(\cos\alpha\hat{\boldsymbol{x}} + \sin\alpha\hat{\boldsymbol{y}})$, where α is the angle between $\boldsymbol{k}_F$ and the x-axis, see Fig. 1. As usual, we work at constant density $n = k_{F0}^2/(4\pi)$, where k_{F0} is the Fermi momentum in the absence of interactions. The chemical potential is then renormalized by the interaction and it is convenient to introduce the interaction-dependent renormalization factor[37]

$$\gamma^2 = \frac{\mu}{E_{F0}} = \frac{2m\mu}{k_{F0}^2}. \tag{22}$$

The self-consistency equation (21) for the Fermi surface can then be written as

$$\frac{k_F(\alpha)}{\gamma k_{F0}} = \sqrt{1 - \frac{\Sigma(k_F(\alpha), 0)}{\mu}}, \tag{23}$$

where $\Sigma(k_F(\alpha), 0)$ is an abbreviation for $\Sigma(k_F(\alpha)[\hat{\boldsymbol{x}}\cos\alpha + \hat{\boldsymbol{y}}\sin\alpha], 0)$. A dimensionless measure for the strength of the interaction is

$$u = 2\pi\nu d^2 k_{F0} = m d^2 k_{F0}, \tag{24}$$

where $\nu = m/(2\pi)$ is the density of states in two dimensions. It is also convenient to introduce the dimensionless ultraviolet cutoff $\Lambda = 1/(k_{F0}\ell)$. Using the parameters realized in the experiment by de Miranda *et al.*[9] for dipolar ^{40}K^{87}Rb in a 2D pancake geometry we work with an approximate density of $n \sim 10^7\text{cm}^{-2}$. Keeping in mind that the size of dipolar molecules is of the order of $\ell \sim 10$Å we estimate $\Lambda \approx 1000$ which we use for our numerical calculations.

Our results for the renormalized Fermi surface are shown in Fig. 4. For sufficiently small interactions the distortion of the Fermi surface can be understood within first order perturbation theory. To this order the renormalized Fermi surface of dipolar fermions in 2D has already been calculated by Chan *et al.*[42]. The Fermi surface stretches along the direction given by the projection of the dipole onto the xy-plane, which is the x-axis

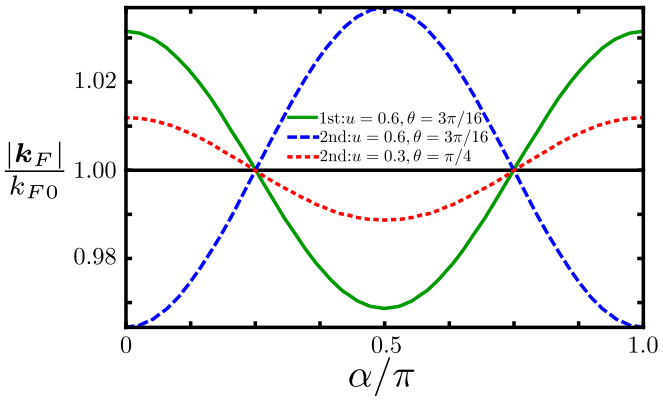

FIG. 4. (Color online) Renormalized Fermi surface in the interval $0 \leq \alpha \leq \pi$ to first and second order in perturbation theory for various choices of u and θ and ultraviolet cutoff $\Lambda = 1/(k_{F0}\ell) = 1000$. The solid green line represents the Fermi surface up to first and the dashed blue line up to second order in the interaction at $u = 0.6$ and $\theta = 3\pi/16$. The dotted red line is the Fermi surface up to second order in the interaction with $u = 0.3$ and $\theta = \pi/4$. The undisturbed Fermi surface is plotted as a reference (solid black line). As we can see, the Fermi surface shows a qualitatively different behavior for certain u and θ in second order perturbation theory. Note that the tilt angle of $\theta = \pi/4$ is above the critical tilt angle for an instability towards the superfluid phase[26,31]; we have choosen this rather large tilt angle for a better visibility of the second order effect at $u = 0.3$.

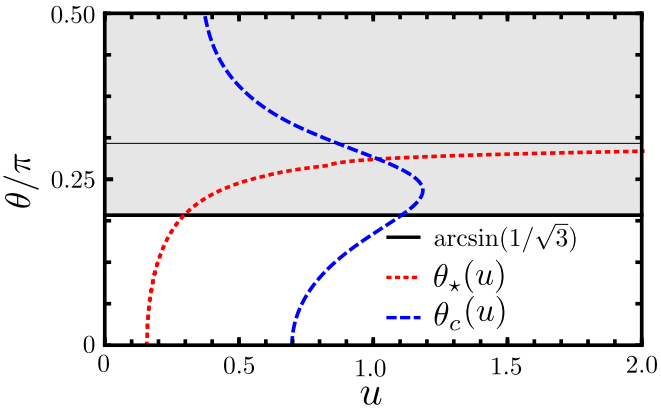

FIG. 5. (Color online) Plot of $\theta_\star(u)$ (red dotted line) and $\theta_c(u)$ (blue dashed line), the critical tilt angle for a vanishing bulk modulus, in full second order perturbation theory. On the left hand side of $\theta_\star(u)$ the Fermi surface is stretched along the x-axes, on the right hand side along the y-axes. As we can see, the Fermi surface changes its elongation before the instability in the density-density channel occurs. The lower horizontal line at $\theta = \arcsin(1/\sqrt{3})$ is approximately the critical tilt angle for an instability towards a superfluid phase[17,31].

with our choice of the coordinate system. Intuitively, this is due to the fact that for finite θ the interaction in real space [Eq. (15)] is most attractive (or, depending on θ, least repulsive) along the x-axis. Therefore particles moving along the x-axis need less energy than particles moving transverse to this axis – hence, the Fermi surface is stretched along the direction defined by the projection of the dipoles on the xy-plane.

The second order correction to the self-energy tends to weaken the first order distortion of the Fermi surface and has the tendency to distort the Fermi surface in a direction that is perpendicular to the projection of the dipoles onto the xy-plane, which is the y-direction with our choice of coordinate system. In fact, if we extrapolate the second order correction to intermediate values of the interaction, the second order correction dominates the first order contribution so that the overall distortion of the Fermi surface is along the y-direction. If we choose the interaction parameter u to be larger than $u_\star \approx 0.15$, we can always find a specific tilt angle $\theta_\star(u)$ of the dipoles such that for $\theta < \theta_\star(u)$ the Fermi surface is distorted along the y-axis. The angle $\theta_\star(u)$ can be defined from the condition that $k_F(\alpha = 0) = k_F(\alpha = \pi/2)$ and is shown as a dotted line in Fig. 5. It would be interesting to investigate whether this effect survives if the interaction is treated non-perturbatively.

Given the renormalized Fermi surface $k_F(\alpha)$, we may determine the renormalized chemical potential $\mu = \gamma^2 E_{F0}$. According to Luttingers theorem[48] the volume enclosed by the Fermi surface gives the particle density n. From the requirement that the particle density must not change when the interaction is turned on we obtain

$$n = \frac{1}{4\pi^2} \int_0^{2\pi} d\alpha \int_0^{k_F(\alpha)} dk k = \frac{k_{F0}^2}{4\pi}. \tag{25}$$

Substituting the self-consistency equation (23) for $k_F(\alpha)$ we obtain

$$\mu = E_{F0} + \frac{2}{\pi} \int_0^{\pi/2} d\alpha \Sigma(k_F(\alpha), 0). \tag{26}$$

Since we do not have analytic expressions for the Fermi momentum we evaluate μ numerically up to u^2. We find

$$\frac{\mu}{E_{F0}} = 1 + f_1(\theta)u + f_2(\theta)u^2 + \mathcal{O}(u^3), \tag{27}$$

where the functions $f_1(\theta)$ and $f_2(\theta)$ are shown in Fig. 6. As we can see $f_1(\theta)$ is positive for small θ which is in the regime where the interaction is mostly repulsive. In contrast, $f_2(\theta)$ is negative for all tilt angles, hence the second order contribution has a destabilizing effect for all θ.

From the renormalized chemical potential we may determine the bulk modulus

$$K = n^2 \left.\frac{\partial \mu}{\partial n}\right|_{V,T}, \tag{28}$$

where the density can be expressed in terms of the bare Fermi momentum as $n = k_{F0}^2/(4\pi)$. We obtain

$$\frac{K}{E_{F0} n} = 1 + \frac{3}{2} f_1(\theta)u + 2 f_2(\theta)u^2 + \mathcal{O}(u^3) \tag{29}$$

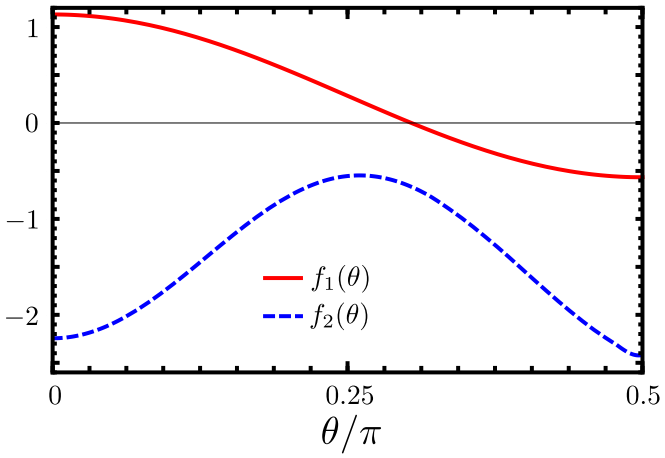

FIG. 6. (Color online) Plot of the functions $f_1(\theta)$ and $f_2(\theta)$ from the perturbative expansion of the renormalized chemical potential and the bulk modulus. The red solid line corresponds to the function $f_1(\theta)$ and the blue dashed line to the function $f_2(\theta)$. Both functions are symmetric around $\theta = \pi/2$. As we can see $f_2(\theta)$ is negative for all tilt angles. Therefore we can always find a critical interaction for which the bulk modulus becomes negative in second order perturbation theory.

with the same functions $f_1(\theta)$ and $f_2(\theta)$ as in Eq. (27), see Fig. 6. Since $f_2(\theta)$ is negative for all tilt angles we can always find a critical interaction in second order perturbation theory for which the bulk modulus becomes negative – even if the interaction is purely repulsive. When the bulk modulus vanishes, the normal state of the system becomes unstable. Using our second order result (29) to estimate the instability regime, we obtain the critical tilt angle $\theta_c(u)$ for vanishing K. The result is plotted in Fig. 5. For $\theta \lesssim \arcsin(1/\sqrt{3})$ our result for the instability line agrees quite well with the result of the random phase approximation for a density-wave instability derived by Yamaguchi *et al.*[21]. The deviation between our critical interaction parameter and the critical interaction derived by Yamaguchi *et al.*[21] depends on the tilt angle, but is not larger than about 15% in the regime $0 \leq \theta \lesssim \arcsin(1/\sqrt{3})$. Note that this instability and the breakdown of second order perturbation theory occur at a much smaller interaction strength than the instability to a stripe phase predicted by Parish *et al.*[31]. Whether our result converges against the critical interaction derived by Parish *et al.*[31] when the interaction is treated non-perturbatively is beyond the scope of this work.

We have also calculated the renormalized Fermi velocity, the quasi-particle residue and the single-particle spectral function of our system. However, in the regime where perturbation theory is valid the corrections are small so that we do not present them here.

IV. SUMMARY AND CONCLUSION

In this work we have calculated the renormalized Fermi surface, the chemical potential, and the bulk modulus in the normal state of two-dimensional dipolar fermions up to second order in perturbation theory. We have pointed out that for idealized point dipoles the second-order self-energy is ultraviolet divergent. To regularize this divergence for electric dipoles, we have replaced the idealized point dipoles by physical dipoles with a finite length ℓ. Our regularization procedure takes all orders in the multipole expansion into account and identifies the ultraviolet cutoff in momentum space with the inverse dipole length. The relevant regime where the dipole length ℓ is large compared with the spatial extend a of the wave function in transverse direction, might at some point be experimentally accessible using dipolar Rydberg atoms or molecules.

While to first order in the interaction the renormalized Fermi surface is always distorted along the direction defined by the projection of the dipoles onto the plane of the system, the second order correction tends to weaken this effect and, for a certain regime of tilt angles θ and dimensionless interaction strengths $u = md^2k_{F0}$, can even change the direction of distortion. From our result for the renormalized chemical potential we have estimated the bulk modulus and the parameter regime where the normal Fermi liquid is stable. The qualitative behavior of our results does not depend on the regularization strategy.

Finally, let us emphasize that we have focussed on electric dipoles because in this case the physical dipoles can be realized as two opposite charges which are separated by a finite distance ℓ. Obviously, our regularization is not valid for magnetic dipoles, however a similar procedure using loop currents seems to be possible but is technically more cumbersome.

ACKNOWLEDGMENTS

We thank the DFG for financial support via FOR 723. We also thank Lorenz Bartosch for useful discussions and inspiring ideas.

[1] J. M. Sage, S. Sainis, T. Bergeman, and D. DeMille, Phys. Rev. Lett. **94**, 203001 (2005).
[2] R. Chicireanu, A. Pouderous, R. Barbé, B. Laburthe-Tolra, E. Maréchal, L. Vernac, J.-C. Keller, and O. Gorceix, Phys. Rev. A **73**, 053406 (2006).
[3] S. Ospelkaus, A. Pe'er, K.-K. Ni, J. Zirbel, B. Neyenhuis, S. Kotochigova, P. Julienne, J. Ye, and D. Jin, Nat. Phys. **4**, 622 (2008).

[4] K.-K. Ni, S. Ospelkaus, M. H. G. de Miranda, A. Pe'er, B. Neyenhuis, J. J. Zirbel, S. Kotochigova, P. S. Julienne, D. S. Jin, and J. Ye, Science **322**, 231 (2008).

[5] S. Ospelkaus, K.-K. Ni, M. de Miranda, B. Neyenhuis, D. Wang, S. Kotochigova, P. Julienne, D. Jin, and J. Ye, Faraday Discuss. **142**, 351 (2009).

[6] J. Deiglmayr, A. Grochola, M. Repp, K. Mörtlbauer, C. Glück, J. Lange, O. Dulieu, R. Wester, and M. Weidemüller, Phys. Rev. Lett. **101**, 133004 (2008).

[7] J. Deiglmayr, A. Grochola, M. Repp, O. Dulieu, R. Wester, and M. Weidemüller, Phys. Rev. A **82**, 032503 (2010).

[8] K.-K. Ni, S. Ospelkaus, D. Wang, G. Quéméner, B. Neyenhuis, M. de Miranda, J. Bohn, J. Ye, and D. Jin, Nature (London) **464**, 1324 (2010).

[9] M. de Miranda, A. Chotia, B. Neyenhuis, D. Wang, G. Quéméner, S. Ospelkaus, J. Bohn, L. Ye, and D. Jin, Nat. Phys. **7**, 502 (2011).

[10] M.-S. Heo, T. T. Wang, C. A. Christensen, T. M. Rvachov, D. A. Cotta, J. H. Choi, Y. R. Lee, and W. Ketterle, Phys. Rev. A **86**, 021602(R) (2012).

[11] C.-H. Wu, J. W. Park, P. Ahmadi, S. Will, and M. W. Zwierlein, Phys. Rev. Lett. **109**, 085301 (2012).

[12] M. Lu, N. Q. Burdick, and B. L. Lev, Phys. Rev. Lett. **108**, 215301 (2012).

[13] M. Repp, R. Pires, J. Ulmanis, R. Heck, E. D. Kuhnle, M. Weidemüller, and E. Tiemann, Phys. Rev. A **87**, 010701 (2013).

[14] K. Aikawa, S. Baier, A. Frisch, M. Mark, C. Ravensbergen, and F. Ferlaino, Science **345**, 1484 (2014).

[15] K. Aikawa, A. Frisch, M. Mark, S. Baier, R. Grimm, and F. Ferlaino, Phys. Rev. Lett. **112**, 010404 (2014).

[16] N. Q. Burdick, K. Baumann, Y. Tang, M. Lu, and B. L. Lev, Phys. Rev. Lett. **114**, 023201 (2015).

[17] G. M. Bruun and E. Taylor, Phys. Rev. Lett. **101**, 245301 (2008).

[18] M. A. Baranov, Phys. Rep. **71**, 464 (2008).

[19] N. R. Cooper and G. V. Shlyapnikov, Phys. Rev. Lett. **103**, 155302 (2009).

[20] B. Fregoso, K. Sun, E. Fradkin, and B. Lev, New J. Phys. **11**, 103003 (2009).

[21] Y. Yamaguchi, T. Sogo, T. Ito, and T. Miyakawa, Phys. Rev. A **82**, 013643 (2010).

[22] C. Zhao, L. Jiang, X. Liu, W. M. Liu, X. Zou, and H. Pu, Phys. Rev. A **81**, 063642 (2010).

[23] R. Liao and J. Brand, Phys. Rev. A **82**, 063624 (2010).

[24] B. M. Fregoso and E. Fradkin, Phys. Rev. B **81**, 214443 (2010).

[25] L. He and W. Hofstetter, Phys. Rev. A **83**, 053629 (2011).

[26] L. M. Sieberer and M. A. Baranov, Phys. Rev. A **84**, 063633 (2011).

[27] B. Liu and L. Yin, Phys. Rev. A **84**, 053603 (2011).

[28] K. Mikelsons and J. K. Freericks, Phys. Rev. A **83**, 043609 (2011).

[29] N. Matveeva and S. Giorgini, Phys. Rev. Lett. **109**, 200401 (2012).

[30] A.-L. Gadsbølle and G. M. Bruun, Phys. Rev. A **86**, 033623 (2012).

[31] M. M. Parish and F. M. Marchetti, Phys. Rev. Lett. **108**, 145304 (2012).

[32] N. T. Zinner, J. R. Armstrong, A. G. Volosniev, D. V. Fedorov, and A. S. Jensen, Few-Body Syst. **53**, 369 (2012).

[33] A. G. Volosniev, J. R. Armstrong, D. V. Fedorov, A. S. Jensen, M. Valiente, and N. T. Zinner, New J. Phys. **15**, 043046 (2013).

[34] B. M. Fregoso and C. A. R. Sá de Melo, Phys. Rev. B **87**, 125109 (2013).

[35] S. G. Bhongale, L. Mathey, S. W. Tsai, C. W. Clark, and E. Zhao, Phys. Rev. A **87**, 043604 (2013).

[36] J. K. Block and G. M. Bruun, Phys. Rev. B **90**, 155102 (2014).

[37] J. Krieg, P. Lange, L. Bartosch, and P. Kopietz, Phys. Rev. A **91**, 023612 (2015).

[38] T. Graß, Phys. Rev. A **92**, 023634 (2015).

[39] G. M. Bruun, C. Hainzl, and M. Laux, arXiv preprint arxiv.org/pdf/1512.01849v1 (2015).

[40] Z. Wu, J. Block, and G. Bruun, Scientific Reports **6**, 19038 (2016).

[41] U. R. Fischer, Phys. Rev. A **73**, 031602 (2006).

[42] C. K. Chan, C. Wu, W. C. Lee, and S. Das Sarma, Phys. Rev. A **81**, 023602 (2010).

[43] C. Ticknor, R. M. Wilson, and J. L. Bohn, Phys. Rev. Lett. **106**, 065301 (2011).

[44] M. Babadi and E. Demler, Phys. Rev. A **86**, 063638 (2012).

[45] M. Babadi, B. Skinner, M. Fogler, and E. Demler, EPL **103**, 16002 (2013).

[46] Instead of representing a physical dipole by point charges, one could alternatively use a continuous smeared out charge density to regularize the interaction, see B. P. van Zyl, E. Zaremba, and P. Pisarski, Phys. Rev. A **87**, 043614 (2013).

[47] *GNU Scientific Library (GSL)*, `http://www.gnu.org/software/gsl/manual/html_node/VEGAS.html`.

[48] J. Luttinger, Phys. Rev. **119**, 1153 (1960).